EPJ Nuclear Sci. Technol. **3**, 27 (2017)

DOI: 10.1051/epjn/2017020

EPJ Nuclear Sciences & Technologies

Available online at:
http://www.epj-n.org

REGULAR ARTICLE OPEN ACCESS

Oxygen segregation in pre-hydrided Zircaloy-4 cladding during a simulated LOCA transient

Elodie Torres[1,*], Jean Desquines[1], Séverine Guilbert[1], Pauline Lacote[1], Marie-Christine Baietto[2], Michel Coret[3], Martine Blat[4], and Antoine Ambard[4]

[1] Institut de Radioprotection et de Sûreté Nucléaire (IRSN), Centre d'Etudes de Cadarache, PSN-RES/SEREX/LE2M, BP3, 13115 Saint Paul-Lez-Durance Cedex, France
[2] INSA de Lyon, Laboratoire de Mécanique des Contacts et des Structures (LaMCoS), UMR 5259, 69621 Villeurbanne Cedex, France
[3] École Centrale de Nantes, Institut de recherche en génie civil et mécanique (GEM), UMR 6183, 44321 Nantes, France
[4] EDF-R&D, Les Renardières, département MMC, 77818 Moret sur Loing, France

Received: 8 December 2015 / Received in final form: 16 May 2017 / Accepted: 8 August 2017

Abstract. Oxygen and hydrogen distributions are key elements influencing the residual ductility of zirconium-based nuclear fuel cladding during the quench phase following a Loss Of Coolant Accident (LOCA). During the high temperature oxidation, a complex partitioning of the alloying elements is observed. A finite-difference code for solving the oxygen diffusion equations has been developed by Institut de Radioprotection et de Sûreté Nucléaire to predict the oxygen profile within the samples. The comparison between the calculations and the experimental results in the mixed α+β region shows that the oxygen diffusion is not accurately predicted by the existing modeling. This work aims at determining the key parameters controlling the average oxygen profile within the sample in the two-phase regions at 1200 °C. High temperature steam oxidation tests interrupted by water quench were performed using pre-hydrided Zircaloy-4 samples. Experimental oxygen distribution was measured by Electron Probe Micro-Analysis (EPMA). The phase distributions within the cladding thickness, was measured using image analysis to determine the radial profile of α(O) phase fraction. It is further demonstrated and experimentally checked that the α-phase fraction in these regions follows a diffusion-like radial profile. A new phase fraction modeling is then proposed in the cladding metallic part during steam oxidation. The modeling results are compared to a large set of experiments including the influence of exposure duration and hydrogen content. Another key outcome from this modeling is that oxygen average profile is straightforward derived from the proposed modeling.

1 Introduction

During a Loss Of Coolant Accident (LOCA), zirconium-based nuclear fuel claddings are submitted to high temperature steam oxidation before core reflooding. During the high temperature oxidation, metallurgical evolutions due to α–β-phase transformations are observed in the material (Fig. 1). A partitioning of the main chemical elements (Sn, Cr, Fe) is also evidenced within the cladding thickness. This segregation is mainly governed by oxygen diffusion and progressive transformation of the β-phase into an oxygen stabilized α(O) layer having a low affinity for these chemical compounds. The microstructure results in a complex distribution of oxygen and hydrogen in the two-phase constituted material.

These phenomena have a direct impact on the material mechanical properties [2]. It was frequently reported that oxygen and hydrogen contents in the prior-β-phase or in the α+β-phase had a combined influence on the cladding post-quenching embrittlement [2–7]. It is thus necessary to understand the mechanisms influencing the motion of these two chemical elements to fully describe the post-quench embrittlement.

Hydrogen distribution within the cladding was previously discussed in another paper [8]. In the open literature, analytical oxygen diffusion models are restricted to samples having simple geometry that is usually not satisfactory for analyzing tubular geometry [9]. A finite-difference software solving the oxygen diffusion equations named DIFFOX (for DIFFusion of OXygen) has been developed by Institut de Radioprotection et de Sûreté Nucléaire (IRSN) [10]. The comparison between the calculations and the experimental results in the mixed α+β region shows that the oxygen diffusion is not accurately predicted. This work aims at

* e-mail: elodietorres@me.com

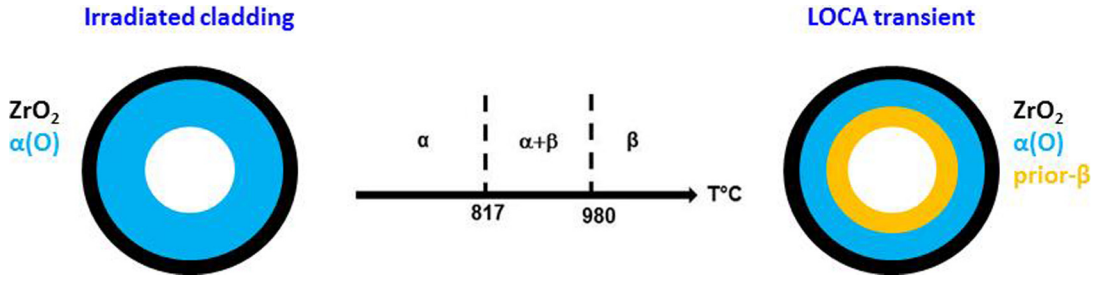

Fig. 1. Metallurgical evolutions of Zircaloy-4 alloy during a LOCA transient [1].

Table 1. Chemical composition of the tested Zircaloy-4.

Sn (wt.%)	Fe (wt.%)	Cr (wt.%)	O (wt.%)	H (wppm)	Zr
1.3	0.21	0.10	0.13	10	Balance

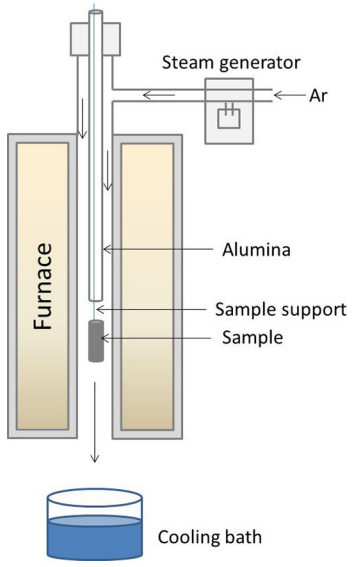

Fig. 2. Vertical furnace used for the steam oxidations at 1200 °C.

determining experimentally the key parameters controlling the average oxygen profile within the sample both in the prior-β-phase and the α+β region at 1200 °C. This study provides improved modeling to be implemented in the diffusion softwares.

Several Zircaloy-4 samples are pre-hydrided with hydrogen contents ranging between the as-received content (~10 wppm) and 400 wppm. The samples are then steam oxidized at high temperature (1200 °C), to simulate LOCA conditions, and then quenched in a water bath at room temperature. The microstructure of the material, especially the phase distributions within the cladding thickness, is systematically characterized by metallography. Local oxygen concentrations are specifically investigated using Electron Probe Micro-Analysis (EPMA). Experimental radial oxygen distributions can then be compared to several diffusion modeling results.

This paper, already published in the proceedings of Topfuel Reactor Performance Conference in Zurich in 2015, describes the test devices and the experimental method supporting this study. The experimental results are presented, discussed and compared to those predicted numerically using calculations derived from the DIFFOX tool. A new modeling is thus proposed. The improved modeling is then validated by comparison to a large set of experiments including influence of exposure duration and hydrogen content.

2 Materials and methods

2.1 Materials

The specimens investigated in this study are stress-relieved annealed low tin Zircaloy-4 fuel cladding tubes fabricated by CEZUS Company. The tubular samples are 70 mm long, have a 9.5 mm outer diameter and a 570 µm thickness respectively. The chemical composition of the tested material is detailed in Table 1.

2.2 Experiments

The 70 mm long specimens are first pre-hydrided at the École Centrale de Paris using gaseous charging at 420 °C. More details about hydrogen gaseous charging are provided in a previous paper [11]. The tubes are then cut into 20 mm long segments for oxidation and thin ring samples both for hydrogen measurements and for metallographic analyses before oxidation. Two-sided steam oxidations are then performed in a vertical furnace at 1200 °C in a mixture of argon and steam. The argon and steam flow rates are respectively 10 Nl min^{-1} and 500 g h^{-1} (50 vol.% argon and 50 vol.% steam) in order to prevent steam starvation and limit hydrogen pick-up. Oxidation durations are adjusted to reach Equivalent Clad Reacted (ECR) values of 15%, 20% and 25% using the Cathcart–Pawel correlation assuming inner and outer diameter oxidation [12]. Oxidation is interrupted by dropping the sample into a water bath at room temperature as illustrated in Figure 2. More details about the oxidation protocol and its qualification are provided by Duriez et al. [10] and Guilbert et al. [13,14].

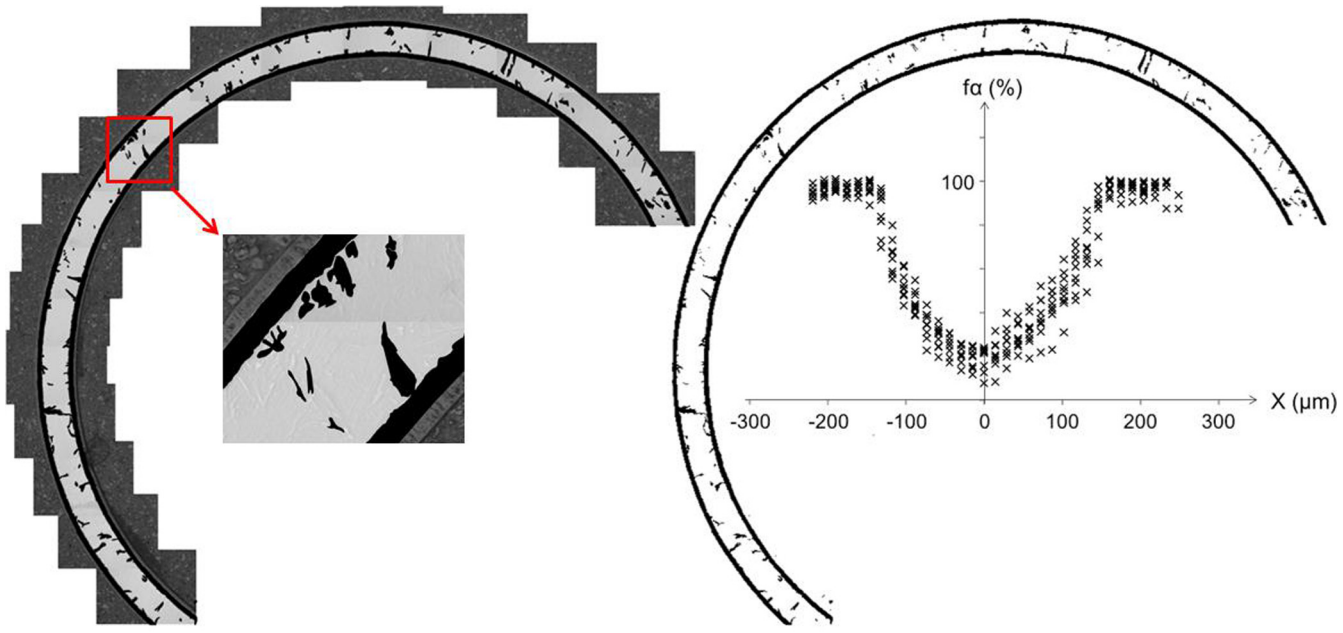

Fig. 3. Example of transformation of the optical metallography into a binary image used to determine the experimental average phase fraction radial profile (sample labelled H66-7).

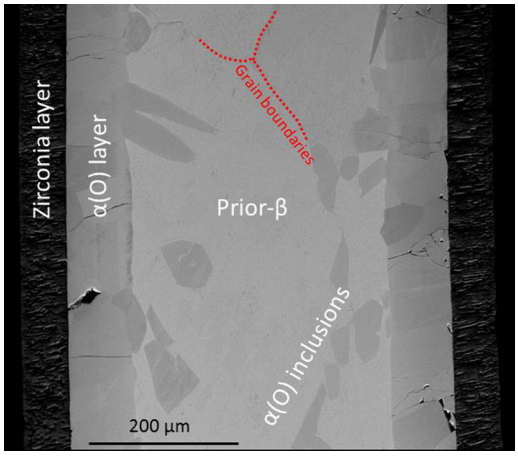

Fig. 4. SEM micrograph of Zircaloy-4 after oxidation at 1200 °C during 400 s (H60-5).

Radial cross sections are prepared for hydrogen measurements and microstructure analyses. Oxygen profiles are systematically measured using EPMA on each radial cut. The microstructure of the material, especially the phase distributions within the cladding thickness, is characterized by metallography.

2.3 Samples characterizations

2.3.1 Hydrogen measurements

The hydrogen content of the samples is measured using a Brücker ONH mat 286 by melting the sample at 2000 °C in the presence of a carrier gas (argon). After calibration, the hydrogen content is determined by catharometry comparing the conductivity of the mixture with the one of pure argon. For 70 mm long tube samples, four axial locations are systematically investigated. A minimum of four analyses at each axial location are performed to check the homogeneity of hydrogen content. After measurement, the zirconia is partially melted in the graphite crucible. Brachet et al. have shown by Elastic Recoil Detection Analysis (ERDA) measurements that the hydrogen content is negligible in the zirconia layer after oxidation at high temperature [15,16]. The zirconia layer weight is thus subtracted to take into account the melted sample weight. Hydrogen is measured after gaseous charging and after steam oxidation.

2.3.2 Metallurgical examinations

After oxidation, two metallographic radial cross sections are cut at each end for all the tested samples. Metallurgical examinations are performed to determine the various material layers thicknesses obtained after the LOCA transient. Oxygen diffusion profiles are investigated by Electron Probe Micro Analysis (EPMA) using a CAMECA SX100 electron probe. Each radial cross section of the samples is embedded in a conductive resin along with an as-received Zircaloy-4 sample. After mechanical polishing, a chemical etching with a hydrofluoric acid solution is performed before introduction into the microprobe vacuum chamber. Oxygen Kα line is measured with a W/Si multi-layer synthetic crystal. Oxygen calibration is performed using as-received Zircaloy-4 with homogeneous and well-known oxygen contents. A typical accuracy of 0.2 wt.% is expected for oxygen content measurements. All the profiles are measured across the thickness with 1 μm stage displacement step in each phase and 250 nm stage displacement step at the zirconia/α(O) and α/prior-β interfaces. Point analyses are also performed in the α(O) inclusions, the α(O) layer and in the prior-β-phase. Maps are obtained from 400 μm × 300 μm areas with a stage displacement step of 1 μm during 300 ms per point.

Table 2. Oxidation results.

Sample (#)	Time s	Initial hydrogen content wppm	Final hydrogen content wppm	ZrO_2 layer thickness μm	α(O) layer thickness μm	Measured ECR %	ECR-CP %	α(O) phase fraction %
AR-1	624	11 ± 5	18 ± 2	71	92	23.6	25	66
AR-2	400	11 ± 5	15 ± 2	58	79	19.6	20	–
AR-3	196	11 ± 5	15 ± 2	44	59	14.7	14	–
H64-3	624	144 ± 17	214 ± 19	74	96	24.2	25	76
H64-5	400	147 ± 17	210 ± 20	59	81	20.2	20	58
H64-7	196	173 ± 24	219 ± 26	44	59	14.9	14	32
H60-3	624	305 ± 39	396 ± 35	72	100	23.8	25	62
H60-5	400	287 ± 32	376 ± 34	58	80	19.0	20	51
H60-7	196	305 ± 38	356 ± 34	42	59	14.1	14	27
H66-3	624	92 ± 12	116 ± 10	74	104	23.9	25	79
H66-5	400	86 ± 9	114 ± 11	57	82	19.8	20	61
H66-7	196	92 ± 12	104 ± 11	43	58	14.3	14	45
H58-3	624	149 ± 17	199 ± 17	68	92	23.8	25	67
H58-5	400	157 ± 18	202 ± 18	58	78	19.7	20	51
H58-7	196	165 ± 18	191 ± 18	43	59	15.1	14	30

Optical microscopy was used to measure the oxide and α(O) layers thickness. The phase distribution in the metallic part of the samples is determined by image analysis based on a half ring metallography reconstruction. The metallography is first transformed into a binary image representing each of the two phases in the metal (Fig. 3). This binary image is then used to determine the average radial profile of α(O) phase fraction $f(\alpha)$. The average profile results from the superposition of several profile measurements at different azimuthal locations assuming constant curvature on a limited angular extension.

3 Results and discussion

3.1 Oxidation results

The typical microstructure of Zircaloy-4 samples after steam oxidation at 1200 °C is illustrated in Figure 4. The measured values of some parameters such as the measured Equivalent Clad Reacted (ECR), initial and final hydrogen contents, α(O) and zirconia layer thicknesses are respectively reported in Table 2. The results indicate low hydrogen pickup during oxidation. A good consistency between measured ECR and its assessment using Cathcart–Pawel correlation is obtained [12]. No influence of hydrogen content on the measured ECR is observed. Hydrogen has no effect on the oxide and oxygen stabilized layer growth. All the results are in agreement with the literature data [2,13,17].

3.2 Oxygen distribution

Oxygen partitioning occurs within the thickness of the cladding tube during the high temperature oxidation. This segregation results from oxygen diffusion inducing a progressive transformation of the β-phase into an oxygen stabilized α(O) layer [18,19]. Oxygen segregation within the cladding samples is systematically analyzed using EPMA. Typical oxygen concentration using point measurements or mapping are illustrated in Figure 5.

Oxygen is segregated into the α-phase consistently with its α-stabilizing properties. Oxygen concentrations are accurately determined by point analysis in each phase. The electron beam is defocused to obtain a lower sensitivity to short-range discrepancies. About 10 measurement points per phase are acquired. Results are plotted in Figure 5b.

3.3 Oxygen concentration profiles modeling

DIFFOX is a 1D finite-difference calculation code describing several connected reaction layers used to solve the oxygen diffusion equations. It has been developed by IRSN to address LOCA induced oxidation [10]. The oxygen concentration profile is calculated by solving the Fick's 2nd law diffusion equation in cylindrical coordinates according to equation (1). The left side is considered to be the oxygen accumulation and the right side the space change of the diffusion flux F_r. The oxygen flux is assumed to be proportional to the oxygen gradient according to the Fick 1st law (Eq. (2)) considering the oxygen in the "n" phase is an ideal mixture. The motion of layer boundaries is derived from the mass balance of oxygen at the interface between two layers according to equation (3). The oxygen diffusion coefficient is extracted from literature data for each of the α(O) phase and β-phase. Considering now the mixed α+β-phase, it is assumed that the oxygen motion is described by a diffusion law applicant to the average oxygen content. Nevertheless, the equivalent diffusion coefficient has to be

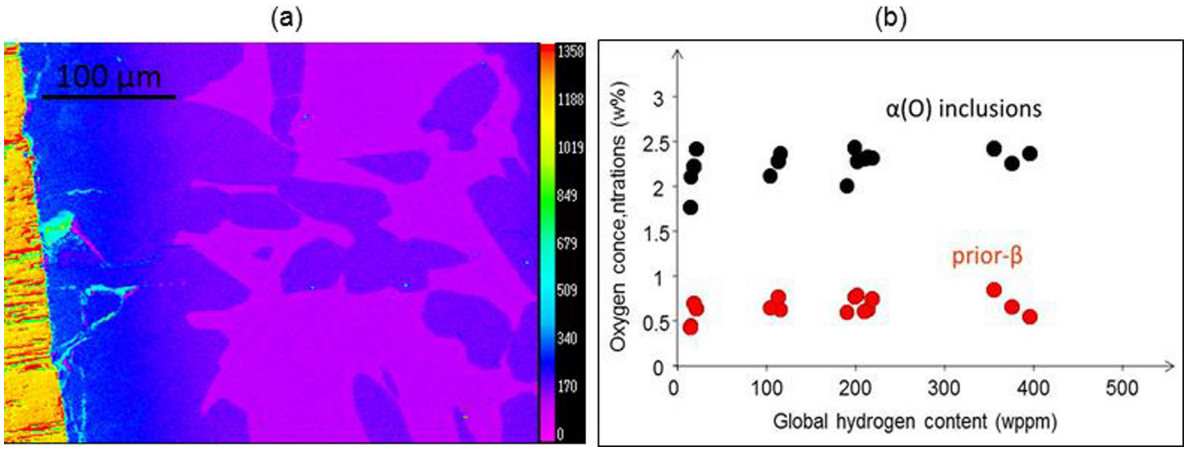

Fig. 5. Oxygen measurements obtained by EPMA of Zircaloy-4 after oxidation at 1200 °C. (a) Maps in the wall cladding the intensity counts is plotted as a color scale (H64-3) and (b) oxygen concentrations in each phase.

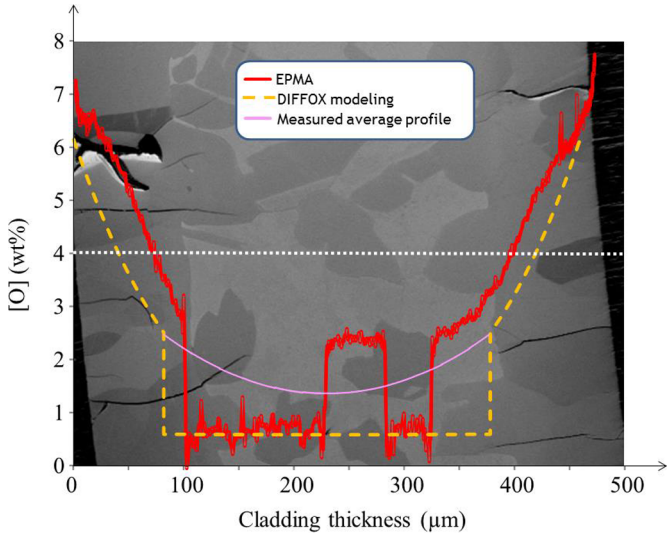

Fig. 6. EPMA oxygen profiles versus DIFFOX calculation or measured average profile (H64-3).

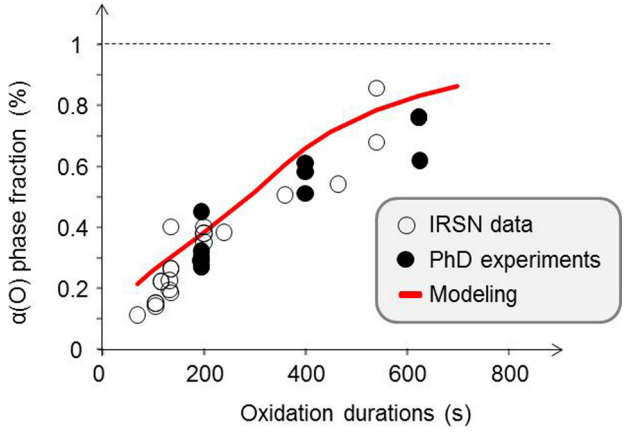

Fig. 7. Measured α(O) average phase fraction versus modeling using numerically determined oxygen diffusion coefficient in the α+β region.

determined. In the DIFFOX code, this diffusion coefficient was empirically determined as well as the conditions required to form a layer containing mixed α+β-phases.

$$\frac{\partial C(r,t)}{\partial t} = \frac{1}{r} \times \frac{\partial}{\partial r}(r \cdot F_r), \tag{1}$$

$$F_r = -D_i(T)\frac{\partial C(r,t)}{\partial r}, \tag{2}$$

where $C(r,\ t)$ is the oxygen concentration, $D_i(T)$ is the oxygen diffusion coefficient in phase i ($i = \alpha,\ \beta,\ \alpha+\beta$), t is the time and r is the radius.

$$\frac{\partial S}{\partial t} = \frac{F_+ - F_-}{2\pi S(C_+ - C_-)}, \tag{3}$$

where S is the interface radius, F_+ and F_- are the left and right side oxygen fluxes, C_+ and C_- the oxygen concentrations at each side of the interface.

Measured oxygen distributions are compared to DIFFOX predictions in Figure 6. The calculations accurately determine the α-layer thickness but strongly underestimate the oxygen content within the α(O) inclusions in the α(O)+β regions. EPMA indicates that in the α(O) inclusions and in the prior-β-phase, the oxygen content is constant but different in each of the two phases. Consequently, the equivalent averaged oxygen radial profile can be determined using the α(O)-phase radial profile. The measurement of oxygen average profile combining EPMA determined concentrations in each phase and average phase radial profile are summarized in equation (4):

$$[O] = C^0_\alpha \cdot f_\alpha + C^0_\beta \cdot f_\beta. \tag{4}$$

A rather continuous oxygen profile is obtained between the α(O) layer and the two-phase region. Experimental and calculated profiles are illustrated in Figure 6. The experimental profile strongly changes in the α+β region depending on the position of inclusions crossed along the

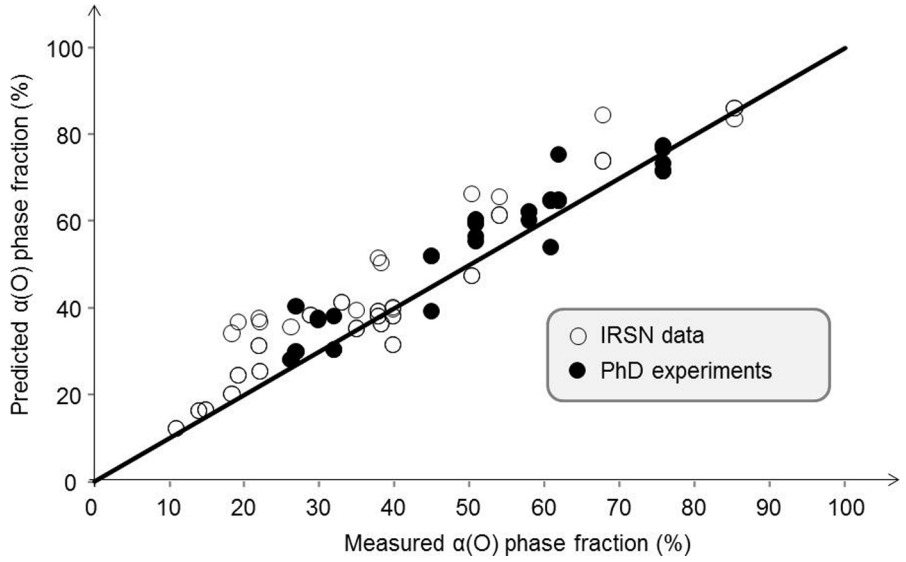

Fig. 8. Comparison between predicted and measured α(O) phase fraction.

radial direction of the performed profile. The calculated profile rather provides an average evolution across the metallic part of the cladding over the entire cross section.

The comparison between the calculations and measurements in the mixed α+β region shows that the oxygen diffusion is not accurately predicted by the modeling tools.

3.4 Oxygen distribution in the two-phase region

Assuming that the oxygen diffusion in the α+β-phase is governed by the Fick 2nd type law, the combined equations (1) and (4) imply that α-phase fraction is also governed by a diffusion-like law having the same diffusion coefficient (Eq. (5)):

$$\frac{df_\alpha}{dt} = D_{\alpha+\beta}\frac{\partial^2 f_\alpha}{\partial r^2}. \tag{5}$$

If the phase fraction is governed by a diffusive process, it is also interesting to consider that equation (5) implies that oxygen distribution follows an equation (1) diffusion type law.

Two types of input data are thus needed for the new calculations: the equilibrium concentration at each interface and the diffusion coefficient in the two-phase region. The oxygen concentrations are relying on EPMA measurements illustrated in Figure 5b.

A Crank analytical solution [20] is first used to determine the concentration profile between the edges of a thick plate having constant concentration at each edge ($r = \pm l$). This solution is used to describe the phase fraction in a cladding having only an α+β region layered by α(O). Indeed, this situation corresponds to long steam exposure at elevated temperature with no remaining β-phase in the central region of the cladding. The boundary layer condition is determined assuming continuity with α(O) uniform layer ($f_\alpha(\pm l, t) = 1$) at the edges of α+β region. The proposed solution is assumed to be acceptably good close to the α/α+β interface and accurate enough for a first order assessment of the oxygen diffusion coefficient $D_{\alpha+\beta}$. The Crank analytical solution [20] is given by equation (6). The diffusion coefficient $D_{\alpha+\beta}$ is adjusted in the solution to fit measured phase fraction profile with the proposed analytical solution:

see equation (6) below

A diffusion coefficient $D_{\alpha+\beta}$ equal to $1.5\times10^{-7}\,\mathrm{cm}^2/\mathrm{s}$ was obtained when simulating the measured radial distribution of phase fraction. As expected, the obtained diffusion coefficient was not did not depend on sample average hydrogen content suggesting that the oxygen diffusion is not influenced by hydrogen.

A new model is developed including a moving interface satisfying the following conditions:

– If the oxygen concentration is lower than the solubility limit in the β-phase, the α(O)-phase fraction is equal to zero and the present study fully relies on literature modeling of oxygen diffusion in the β-phase. Oxygen diffusion is thus homogeneous in this phase and governed by equation (7) with D_β is equal to $1.6\times10^{-6}\,\mathrm{cm}^2/\mathrm{s}$ [21].

$$\frac{d[O]}{dt} = D_\beta\frac{\partial^2[O]}{\partial r^2}. \tag{7}$$

– If the oxygen concentration in the β-phase reaches the solubility limit, the phase fraction increases at the considered location and follows equation (8). In this

$$f_{\alpha(r,t)} = \frac{4}{\pi}\sum_{n\geq 0}\left[\frac{-1^n}{2n+1}\exp\left(-\frac{D_{\alpha+\beta}(2n+1)^2n^2t}{4l^2}\right)\cos\left(\frac{(2n+1)\pi r}{2l}\right)\right]. \tag{6}$$

situation, the oxygen concentration in both the α(O) inclusions and the prior-β-phase are determined relying on EPMA measurements (Fig. 5). The link between phase fraction and oxygen content is established by equation (4). The inclusion growth is then controlled by grain boundary diffusion of oxygen along the α(O) inclusion interface with β-phase as described by equation (8) where $D_{\alpha+\beta}$ is an empirical overall diffusion coefficient for the two-phases layer:

$$\frac{df_\alpha}{dt} = D_{\alpha+\beta}\frac{\partial^2 f_\alpha}{\partial r^2}. \quad (8)$$

In other words, the oxygen diffusion follows the $\frac{d[O]}{dt} = D_{\alpha+\beta}\frac{\partial^2[O]}{\partial r^2}$ diffusion equation.

– The $\alpha/\alpha+\beta$ interface motion is governed by equation (9) using experimental measurements for both α(O) and zirconia layer thicknesses.

$$r_{\text{interface}} = \alpha(\text{O})_{\text{measured}} + \frac{1}{1.56}\text{e}_{\text{zirconia(measured)}} \quad (9)$$
$$\text{and } f_\alpha(r_{\text{interface}},\, t) = 1,$$

where $\text{e}_{\text{zirconia}}$ is the measured oxide layer thickness and 1.56 is the Pilling–Bedworth ratio for transformation of zirconium into zirconia.

A good consistency between the average phases fractions measured across the sample metallic surfaces versus oxidation time is obtained for a $D_{\alpha+\beta}$ value of $1.5\times10^{-7}\,\text{cm}^2/\text{s}$ as illustrated in Figure 7. Experiments obtained in this study but also from previous experiments conducted at IRSN with identical material are then simulated in order to validate this approach in the $\alpha+\beta$ regions. A good consistency is obtained between measured and predicted α(O)-phase fraction as illustrated in Figure 8.

4 Conclusions and perspectives

The present study addresses oxygen distribution in Zircaloy-4 cladding after a LOCA steam oxidation transient. Within the samples, special attention was paid to the region with co-existing $\alpha(\text{O})+\beta$-phases. This region is not homogenous and considering 1D diffusion modeling, a special data treatment has to be performed to compare experimental data to modeling results. Using EPMA measurements, oxygen distribution within the cladding samples after steam oxidation was better characterized. Average radial profiles of oxygen have been determined assuming that the phase contents are uniform and close to equilibrium conditions. The oxygen profile is compared to diffusion simulations using the DIFFOX tool. The model prediction has shown that oxygen diffusion in the mixed phase region has to be improved. A new modeling was consequently proposed to determine the oxygen diffusion mechanisms in the two-phase region. The modeling results are satisfactorily compared to a large set of experiments. This model has been only fitted and validated at 1200 °C and should be further tested at other oxidation temperatures.

References

1. H.M. Chung, T.F. Kassner, Pseudobinary Zircaloy-oxygen phase diagram, J. Nucl. Mater. **84**, 327 (1979)
2. J.-C. Brachet et al., Hydrogen content, peroxidation, and cooling scenario effects on post-quench microstructure and mechanical properties of Zircaloy-4 and M5® alloys in LOCA conditions, J. ASTM Int. **5**, JAI101116 (2008)
3. J.C. Brachet et al., Influence of hydrogen content on the α/β-phase transformation and on the thermal–mechanical behavior of Zy-4, M4 and M5 alloys during the first phase of LOCA transient, in *Zirconium in the Nuclear Industry: 13th International Symposium, ASTM-STP 1423, Annecy, France* (2001), pp. 673–701
4. N. Waeckel, Fuel safety research at EDF, in *FSRM Meeting, Tokyo* (2005)
5. M. Billone, Y. Yan, T. Burtseva, R. Daum, Cladding embrittlement during postulated Loss-of-Coolant Accidents, NUREG-CR-6967, US-NRC, 2008
6. A. Sawatsky, A proposed criterion for the oxygen embrittlement of Zircaloy-4 fuel cladding, in *Zirconium in the Nuclear Industry: 4th International Symposium, ASTM STP 681* (1979), pp. 479–496
7. A.M. Garde, H.M. Chung, T.F. Kassner, Uniaxial tensile properties of Zircaloy containing oxygen, ANL Report 77-30, 1977
8. E. Torres, J. Desquines, M.-C. Baietto, M. Coret, F. Wehling, M. Blat-Yrieix, A. Ambard, Adsorption and diffusion of hydrogen in Zircaloy-4, Fontevraud 8 – Contribution of Materials Investigations and Operating Experience to LWRs' Safety, Performance and Reliability, paper 198-T09-FP, 2014
9. X. Ma, C. Toffolon-Masclet, T. Guilbert, D. Hamon, J.C. Brachet, Oxidation kinetics and oxygen diffusion in low-tin Zircaloy-4 up to 1523 K, J. Nucl. Mater. **377**, 359 (2008)
10. C. Duriez et al., Characterization of oxygen distribution in LOCA situations, J. ASTM Int. **8**, 2 (2010)
11. E. Torres, J. Desquines, S. Guilbert, M.-C. Baietto, M. Coret, P. Berger, M. Blat-Yrieix, A. Ambard, Hydrogen motion in Zircaloy-4 cladding during a LOCA transient, in *Ic-cmtp3 International Conference* (2014)
12. J.V. Cathcart, R.E. Pawel, R.A. McKee, R.E. Druschel, G.J. Yurek, J.J. Campbell, S.H. Jury, Zirconium metal-water oxidation kinetics IV. Reaction rate studies, NRC report ORNL/NUREG-17, 1977
13. S. Guilbert, C. Duriez, C. Grandjean, Influence of a pre-oxide layer on oxygen diffusion and on postquench mechanical properties of Zircaloy-4 after steam oxidation at 900 °C, in *Proceedings of 2010 LWR Fuel Performance/TopFuel/WRFPM, Orlando, Florida, USA, September 26–29*, 2010 – Paper 121 (2010)
14. S. Guilbert et al., Effect of pre-oxide on Zircaloy-4 high-temperature steam oxidation and post-quench mechanical properties, ASTM STP 1523, 2013
15. C. Raepsaet, P. Bossis, D. Hamon, J.L. Béchade, J.C. Brachet, Quantification and local distribution of hydrogen within Zircaloy-4 PWR nuclear fuel cladding tubes at the nuclear microprobe of the Pierre Süe Laboratory from μ-ERDA, Nucl. Instrum. Methods Phys. Res. Sect. B **266**, 2424 (2008)
16. J.C. Brachet et al., Oxygen, hydrogen and main alloying chemical elements partitioning upon alpha–beta phase transformation in zirconium alloys, Solid State Phenom. **172–174**, 753 (2011)

17. M. Le Saux et al., Influence of pre-transient oxide on LOCA high temperature steam oxidation and postquench mechanical properties of Zircaloy-4 and M5^{TM} cladding, Water Reactor Fuel Performance Meeting, paper T3-040, 2011
18. C. Toffolon-Masclet, C. Desgranges, C. Corvalan-Moya, J.-C. Brachet, Simulation of the $\beta \rightarrow \alpha$(O) phase transformation due to oxygen diffusion during high temperature oxidation of zirconium alloys, Solid State Phenom. **172**, 652 (2011)
19. J.C. Brachet et al., Mechanical behavior at room temperature and metallurgical study of low-Tin Zy-4 and M5^{TM} after oxidation at 1100 °C and quenching, in *Proc. of TCM on Fuel behavior under transient and LOCA conditions*, IAEA, Halden-Norway, September 10–14 (2001)
20. J. Crank, *The Mathematics of Diffusion*, 2nd edn. (Oxford University Press, Ely House, London, 1975)
21. R.A. Perkins, Oxygen diffusion in β-zircaloy, JNM **68**, 148 (1977)

Cite this article as: Elodie Torres, Jean Desquines, Séverine Guilbert, Pauline Lacote, Marie-Christine Baietto, Michel Coret, Martine Blat, Antoine Ambard, Oxygen segregation in pre-hydrided Zircaloy-4 cladding during a simulated LOCA transient, EPJ Nuclear Sci. Technol. **3**, 27 (2017)